Attosecond angular streaking

PETRISSA ECKLE[1]*, MATHIAS SMOLARSKI[2†], PHILIP SCHLUP[1‡], JENS BIEGERT[1†], ANDRÉ STAUDTE[2§], MARKUS SCHÖFFLER[2], HARM G. MULLER[3], REINHARD DÖRNER[2] AND URSULA KELLER[1]

[1]Department Physik, ETH Zurich, Wolfgang-Pauli-Str. 16, 8093 Zurich, Switzerland
[2]Institut für Kernphysik, Johann Wolfgang Goethe Universität, Max-von-Laue-Str. 1, 60438 Frankfurt am Main, Germany
[3]FOM-Institute for Atomic and Molecular Physics, Kruislaan 407, 1098 SJ Amsterdam, The Netherlands
[†]Current Address: ICFO-Institut de Ciencies Fotoniques, Mediterranean Technology Park, 08860 Castelldefels (Barcelona), Spain
[‡]Current Address: Colorado State University, Fort Collins, Colorado 80523, USA
[§]Current Address: Steacie Institute for Molecular Sciences, National Research Council of Canada, 100 Sussex Drive, Ottawa, Ontario K1A 0R6, Canada
*e-mail: eckle@phys.ethz.ch

Published online: 30 May 2008; doi:10.1038/nphys982

Ultrashort measurement-time resolution is traditionally obtained in pump–probe experiments, for which two ultrashort light pulses are required; the time resolution is then determined by the pulse duration. But although pulses of subfemtosecond duration are available, so far the energy of these pulses is too low to fully implement the traditional pump–probe technique. Here, we demonstrate 'attosecond angular streaking', an alternative approach to achieving attosecond time resolution. The method uses the rotating electric-field vector of an intense circularly polarized pulse to deflect photo-ionized electrons in the radial spatial direction; the instant of ionization is then mapped to the final angle of the momentum vector in the polarization plane. We resolved subcycle dynamics in tunnelling ionization by the streaking field alone and demonstrate a temporal localization accuracy of 24 as r.m.s. and an estimated resolution of ≈200 as. The demonstrated accuracy should enable the study of one of the fundamental aspects of quantum physics: the process of tunnelling of an electron through an energetically forbidden region.

Discoveries in high-field physics reduced the available pulse duration of light pulses from the few-femtosecond regime[1] in 1999 to the first attosecond pulses in 2001 (refs 2,3), to most recently 130 attoseconds[4]. By combining attosecond pulses with femtosecond infrared electric-field streaking (an approach known as 'energy streaking')[5], subfemtosecond time resolution has been achieved for the first time.

Angular streaking has been proposed some years ago[6] as a single-shot measurement technique for the carrier envelope offset phase (ϕ_{CEO}) of few-cycle pulses; however, so far no experimental results have been obtained. The rotating electric-field vector of the circularly polarized pulse is used to deflect photo-ionized electrons in the angular spatial direction, such that the instant of ionization is mapped to the final angle of the momentum vector in the polarization plane—similar to the minute hand of a clock. In our case, this 'atto-clock' runs over one 360° turn of the electric field in 2.4 fs. It requires pulse durations in the two-optical-cycle regime and carrier-envelop-phase (CEP) control.

Attosecond dynamics have previously been measured by other methods. A 100 as measurement accuracy was achieved by mapping time to frequency via the known frequency chirp of the short-trajectory harmonic emission—also without the need for attosecond pulses[7]. More closely related to angular streaking is energy streaking[5] that uses a linearly polarized infrared field to map time to energy[8], whereas angular streaking uses circularly polarized infrared light to map time to angle. In energy streaking an attosecond pump pulse generates photoelectrons that are then accelerated by a linearly polarized infrared laser field. This streaking field determines the final kinetic energy of the photoelectrons depending on their time of ionization, so time is mapped to energy[8]. Using this approach, the electric field of a few-cycle pulse was measured with a temporal resolution of 200 as (ref. 9).

There are different trade-offs between angular and energy streaking. One advantage of angular streaking is that we do the streaking over one full cycle, whereas energy streaking is limited to about a quarter of a cycle where the electric field changes approximately linearly with time[10]. In addition, angular streaking has the extra option to use only the infrared electric field to study attosecond dynamics. In energy streaking, an attosecond pulse is required because the streaking electric field alone would tunnel ionize the atoms at the peak of the field where no energy streaking is taking place. Thus, the short event needs to be confined to the lower electric-field strength where the streaking infrared pulse cannot (and should not) induce ionization. Thus, the temporal resolution is limited to the attosecond pulse duration. Currently, the shortest pulse duration is at 130 as, which is already in the single-extreme-ultraviolet-cycle regime[4]. The resolution of angular streaking is limited by the angular spread of the photoelectron wave packet, which is not the case for energy streaking[5]. This resolution limit will be strongly reduced if angular streaking is combined with an attosecond extreme-ultraviolet pulse. Using only the infrared electric field in angular streaking, and not an attosecond extreme-ultraviolet pulse as well, is in our opinion a real advantage to study, for example, tunnelling dynamics. More recently, double ionization dynamics have been observed with a combination of energy streaking and infrared-induced tunnel ionization of highly excited Ne^+ atoms[12]. The overall temporal resolution was limited to ≈380 as and CEP-dependent steps in tunnelling ionization of Ne^+ indicated a ≈100 as resolution. In that case, the tunnelling time was not measured alone. The response is a

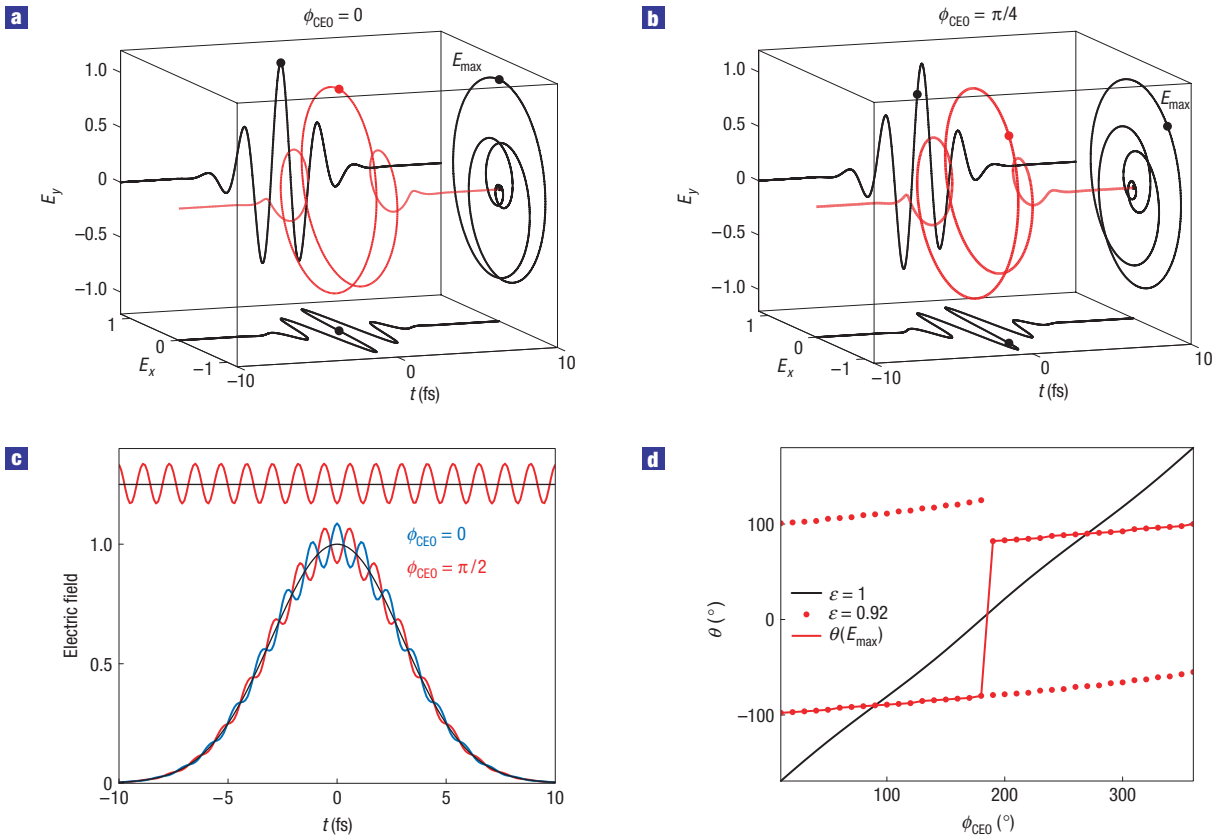

Figure 1 CEP in circularly and elliptically polarized few-cycle pulses. a,**b**, Evolution of the electric field $E(t)$ of a circularly polarized few-cycle pulse for a fixed position on the propagation axis with the field maximum E_{max} indicated by a dot. In the absence of temporal chirp, the electric field at a fixed position in space along the propagation direction will rotate at the optical centre frequency with increasing and then decreasing amplitude. The electric field (red) can be written as a sum of two orthogonal components (black) that differ in the CEP ϕ_{CEO} by $\pi/2$, $E_x(t) = E_{0x}(t)\cos(\omega_0 t + \phi_{CEO})$ and $E_y(t) = E_{0y}(t)\cos(\omega_0 t + \phi_{CEO})$, with equal temporal pulse envelopes $E_{0x}(t) = E_{0y}(t)$. The CEP in **b** is shifted by $\pi/4$ compared with that in **a**. **c**, For elliptical polarization ($E_{0x}(t) \neq E_{0y}(t)$), the corresponding magnitude of the electric field, $E(t) = \sqrt{E_x^2(t) + E_y^2(t)}$, varies with time. The black line shows the envelope for circular polarization; the blue and red curves correspond to an ellipticity of 0.92 (with a relative CEP shift of $\pi/2$). The ellipticity is defined by the ratio $E_{0x}(t)/E_{0y}(t)$ assuming $E_{0x}(t) < E_{0y}(t)$. In elliptical polarization, the peak of the electric-field vector rotates along an ellipse with a maximum and minimum electric-field magnitude separated by 90° (a period of 180°). Shifting the CEP in this case moves the pulse envelope through the subcycle oscillations, creating one dominant peak on the field evolution if the maximum of the pulse envelope points in the direction of the major axis of the ellipse (blue line), and two equal smaller peaks if it points in the direction of the minor axis (red line). For a two-cycle pulse duration, this subcycle oscillation period is weakly CEP dependent. **d**, The angular mapping of the azimuthal coordinate angle θ for the spatial orientation of the maximum of the electric field E_{max} as a function of the CEP for circular polarization (black) and an ellipticity of 0.92 (red circles). In the latter case, we emphasize the absolute maximum with a solid red line.

sum of the excitation and tunnelling time, and the overall dynamics are very complex.

In angular streaking, we have to distinguish between two different parameters that describe the temporal limitations: temporal localization (tracking the peak of the ionization rate) and resolution (minimum time difference to separate two different ionization events). It is a common problem in experimental data analysis to locate the peak position of a signal to an accuracy, which is substantially better than the actual signal width[13]. The longer the acquisition time, the better the localization accuracy as long as no systematic errors occur. Thus, in principle, arbitrarily high accuracy can be achieved. This has been demonstrated both in high-resolution spectroscopy and high-resolution spatial imaging. For example, molecular motion has been resolved with a 1.5 nm localization accuracy[14] even though the point-spread function is much wider. It is possible to follow molecular movements with 2–3 nm spatial localization accuracy even though their spatial image width is of the order of 200–300 nm. Analogous results are reported in high-resolution spectroscopy. Here, we have demonstrated a temporal localization accuracy that potentially enables unique measurements discussed later.

CEP EFFECTS IN ANGULAR STREAKING

For the angular streaking method, we must stabilize the pulse's electric-field evolution to a known circular polarization state in space (Fig. 1a,b). With CEP stabilization[15–17], the maximum electric-field vector is fixed in space and its angle does not change from pulse to pulse. Changing the CEP will rotate this position in space along with the entire electric-field evolution of the pulse[18] (Fig. 1a,b, Supplementary Information, Movie S1). For perfectly circularly polarized pulses, the time-dependent magnitude of the electric-field vector does not depend on the CEP (Fig. 1c). Thus, in circularly polarized light, the CEP is only an angular offset to the 'atto-clock'. In the few-cycle regime, however, it is in practice difficult to generate perfectly circularly polarized light owing to

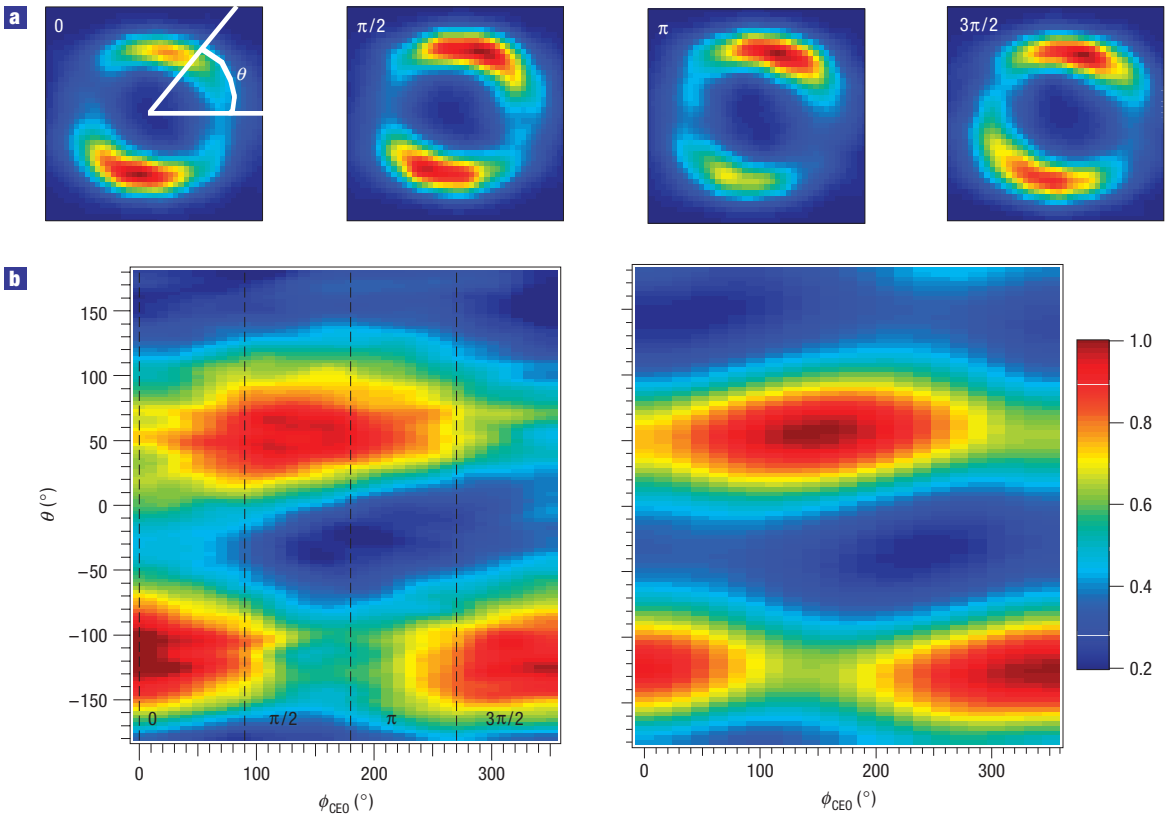

Figure 2 Overview of the measured helium-ion momentum distributions while scanning the CEP over 2π and comparison with a semiclassical simulation. **a**, Toroidal He^+ momentum distributions projected onto the *xy* polarization plane for four different CEP values $\phi_{CEO} = 0, \pi/2, \pi$ and $3/2\pi$, respectively. **b**, Radially integrated distributions as a function of CEP ϕ_{CEO} for the entire CEP scan (left) compared with simulations (right).

the large spectral bandwidth. A minor amount of ellipticity results in subcycle oscillations on top of the electric-field envelope with a period of approximately half the optical cycle of the carrier field (Fig. 1c).

Without CEP stabilization, these field modulations are completely obscured in the time domain. However, the modulations in the field remain spatially observable because the main axes of the polarization ellipse do not depend on the CEP (Fig. 1d). These oscillations become the dominant feature in the tunnel ionization rates even for very small deviations from perfectly circular light (ellipticity = 0.99) owing to the high nonlinearity of the process. The angular streaking, in contrast, is not strongly affected because it depends linearly on the electric field. For an actual attosecond streaking measurement, the CEP is set to a constant value and the ultrafast dynamics are mapped in space with a fixed temporal scale. This scale can be measured with very high accuracy using well-established characterization tools to determine amplitude and phase of the infrared streaking field—such as, for example, spectral phase interferometry for direct electric-field reconstruction[19] (SPIDER).

ACCURACY AND RESOLUTION OF THE ATTO-CLOCK

For a first demonstration of attosecond angular streaking, we have measured the ion momentum space distribution of helium ionized with intense CEP-controlled, near-circularly polarized 5.5 fs infrared pulses compressed by a two-stage filament compressor[20] centred at 725 nm and a cycle duration of 2.4 fs (see Methods section). The momentum distributions were measured with a cold-target recoil-ion momentum spectrometer[21] (COLTRIMS). The helium atoms are ionized in the tunnelling regime with a Keldysh parameter $\gamma \approx 1.17$ (ref. 11), well below the saturation intensity, such that the ionization probability is only dependent on the instantaneous electric-field strength. The process can be described in two steps in analogy to the well-known three-step model[22]. In the first step, the electrons tunnel through the atomic potential barrier that is lowered by the electric field of the pulse. The ions and electrons are subsequently accelerated by the pulse field and deflected from the direction of the electric field at the instant of ionization by approximately 90° according to the vector potential at that instant that shows a phase shift of 90° compared with the field. The final momentum distribution then has a toroidal shape around the laser propagation direction (Fig. 2a). Momentum conservation ensures that for single ionization the electron and ion momentum distributions are identical.

Measured momentum distribution results are shown in Fig. 2. As expected, the slight ellipticity in our infrared pulses is enhanced in the ion count rate through the high nonlinearity of the ionization process and leads to two pronounced peaks in the angular momentum distributions. The two peaks on the angular momentum distributions change in relative intensity but are only weakly angle-shifted with changing CEP because the spatial orientation of the ellipticity axis does not change with the CEP (Figs 2a,b and 1d).

To specify the temporal localization accuracy, we determined the angular positions of the peaks of the subcycle oscillations on the

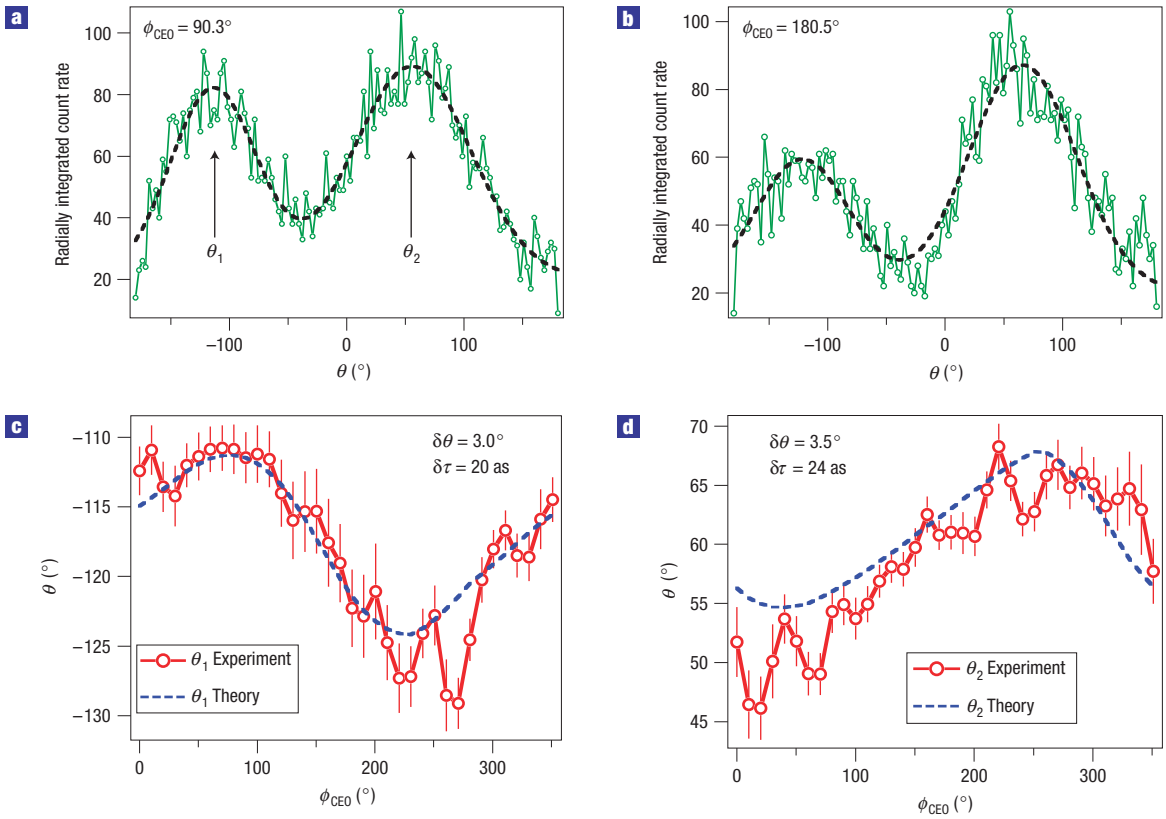

Figure 3 CEP dependence of the ionization angle in He using attosecond angular streaking. a,**b**, Radially integrated ion momentum distributions as shown in Fig. 2b (left). The double peak structure is clearly resolved within a measurement span of one optical cycle (2.4 fs or 360° streaking angle span) for two different but constant CEP values. The dashed curve corresponds to a double gaussian fitting function that determines the streaking angle and the error for the two peaks in the momentum distribution: θ_1 and θ_2. **c**,**d**, The angular position of the two peaks θ_1 and θ_2 as a function of the CEP ϕ_{CEO} measured (red) and simulated (blue). The error bars show the r.m.s. error of the double gaussian fit applied to the individual data sets as shown in **a**,**b**. The r.m.s. error in the measured data of 24 as follows from the comparison with the theoretical curve.

measured momentum distributions, and compared them with our semiclassical simulation (see the Methods section). The results are shown in Fig. 3. For each value of the CEP, the radially integrated angular distribution is fitted with a double gaussian function to extract the angular location of the peaks within one optical cycle. Figure 3a,b shows this fit for two different CEP settings. The r.m.s. error of the maxima of each of the two ionization peaks is less than 3.5° or ≈24 as (Fig. 3a,b). The same procedure was applied to the simulated momentum distributions. The r.m.s. error for the full data set compared with the theoretical simulations for both oscillation peaks was 24 as (Fig. 3c,d). This confirms that the semiclassical model describes this ionization process with sufficient accuracy. With this measurement, we have demonstrated that attosecond angular streaking can be used to track photo-ionization dynamics with high temporal localization accuracy. The two ionization rate oscillation peaks (for example, Fig. 3a,b) are fully resolved, which means that our temporal resolution does not limit this measurement because the subcycle oscillation period is much longer than the resolution. We therefore need to make an estimation for the ultimate temporal resolution.

We applied two theoretical models to estimate the ultimate temporal resolution. Both predicted a resolution in the range of 200 as. Our semiclassical model based on Ammosov–Delone–Krainov (ADK) tunnelling theory[23] would predict a temporal resolution of ≈160 as assuming a classical electron trajectory after tunnelling (see the Methods section). A full quantum mechanical model based on the time-dependent Schrödinger equation would predict a maximum resolution of ≈230 as at our infrared frequency (see the Methods section). A classical trajectory calculation can show that the residual Coulomb interaction on the escaping electron is very small (less than 5°) for our condition.

SIMULATION DETAILS

For our semiclassical simulation, we calculated the ionization probability and initial momentum of photoelectrons from He atoms with the ADK formalism[24]. The electrons were propagated classically in the calculated pulse field. The final momentum distribution was obtained by calculating an ensemble of traces in momentum space. The starting times were chosen in a range of 10 fs centred on the field maximum in steps of 0.01 fs. For each starting time, 400 traces were calculated and the initial velocity was chosen to match the momentum distribution predicted by the ADK theory. To match the experimental conditions, an initial thermal distribution of 2.8 K in the jet was included.

For the temporal resolution estimate, we integrated the time-dependent Schrödinger equation for a helium atom in a circularly polarized infrared field peak intensity of 100 TW cm^{-2}, while putting a pulsed source of electrons on the nucleus. This source term was designed to emit electrons in the same direction as for infrared-induced tunnelling by populating a suitably chosen superposition of the threshold *p*-wave and *d*-wave. It could be

switched on and off rapidly without non-adiabatic effects on the wavefunction inside the atomic potential well. This is different to any other attempts to quickly switch on a tunnelling current with a short high-energy electric-field wave packet. With this approach, we determined the narrowest angular spread of the free electrons to be 35° full-width at half-maximum, corresponding to a resolution of ≈230 as at our central infrared frequency. This resolution was obtained with an electron source assuming a gaussian switching pulse of 93 as full-width at half-maximum. The attempt to measure even shorter events by confining ionization to ever shorter times leads to a wider angular spread in the streaked wave packet due to the higher spread of ejection energies.

POTENTIAL TO MEASURE TUNNELLING TIME

Interestingly, the temporal localization accuracy that we have demonstrated opens the possibility to examine one of the fundamental aspects of quantum physics: the process of tunnelling of a particle through an energetically forbidden region. Theory maintains that tunnelling through a forbidden region is associated with a real time, a traversal time[25,26] for tunnelling. Indeed, our temporal localization accuracy is in the range of the fundamental tunnelling traversal time Δt, which can be estimated by $\gamma = \omega_0 \Delta t$ (atomic units), where γ is the Keldysh parameter and ω_0 is the centre laser angular frequency. For our experiment, this would result in a tunnelling time of ≈400 as, well within our temporal localization accuracy.

The tunnelling time results in an angular offset of the entire momentum distribution. We used a two-dimensional fitting procedure with regard to the CEP and the angular streaking angle in Figs 2 and 3 to compare the raw data as shown in Fig. 2b (left) with a semiclassical simulation (Fig. 2b (right)). To measure this angular offset, an extra independent measurement for the absolute angular position of the electric field (the absolute CEP) is necessary. In our current experiment, we have not implemented such a measurement and therefore determined the CEP in comparison with our ionization rate measurement neglecting any extra shift due to a possible tunnelling time. We measured this CEP with the temporal localization accuracy of 24 as, which corresponds to 0.06 rad. This accuracy is comparable to other CEP measurements[27,28], but in principle can be improved for longer acquisition times.

In summary, we have measured a 24 as temporal localization of the photo-ionization in He over a measurement span of 2.4 fs using attosecond angular streaking with an infrared field alone. The predicted resolution for a single ionization event of ≈200 as is essentially only limited by quantum mechanics through the angular spread of the tunnelling wave packet. Subcycle ionization dynamics have been clearly resolved, and we were able to track the temporal movement of the ionization peaks induced by ramping the CEP through ≈2π. A 24 as temporal localization of this movement and an excellent agreement with a semiclassical model has been achieved. This measurement technique does not necessitate attosecond pulses, which are currently limited to 130 as and technically very demanding to generate and use. The necessary 'time zero' that would be provided by the attosecond pulse can, in the case of angular streaking using infrared fields alone, be replaced by an independent *in situ* measurement of the absolute phase, for example, by a phase meter (Stereo-ATI (ref. 27) or in the COLTRIMS directly). Combining angular streaking with attosecond extreme-ultraviolet pulses opens up other possibilities, such as, for example, attosecond pulse characterization as proposed in refs 29,30. Angular streaking has the potential to time resolve multi-electron processes, such as shake-off and sequential double ionization with attosecond time resolution. When we combine attosecond angular streaking with state-of-the-art multi-electron detection techniques, we are able to record the timing sequence of several steps in a few-electron process by mapping the time of one electron to an angle in space and the time difference between subsequent ionization events to angular differences. These measurements have the potential to reveal deeper insight into possible electron correlation effects in the timing difference of the individual tunnelling ionization events of two electrons. In addition, we expect that the time resolution in a modified molecular-clock experiment can be improved substantially, using the angle between two electrons generated in sequential double ionization to accurately measure the instants of ionization (see Methods section). For a single tunnelling event, we are limited by the temporal localization accuracy, which opens up the exciting possibility to measure electron tunnelling time directly. This temporal localization can in principle be improved to arbitrarily high precision by collecting a sufficiently large number of photo-ionized electron or ion counts as long as no systematic error occurs. Our current temporal localization accuracy is not limited in this regard and we hope to further improve this result. Tunnelling time is a very fundamental quantum physics phenomenon and is important for many different fields (for example, high-field physics, nanostructures and superconductors). Tunnelling time has been an ongoing controversial discussion over the past 60 years: theory maintains that tunnelling through a forbidden region is associated with a real time.

METHODS

EXPERIMENTAL SET-UP DETAILS

Linearly polarized 5.5 fs pulses were generated from 30 fs pulses in a two-stage filament compressor. During filamentation, the centre wavelength shifted to 725 nm and the spectrum is deformed. The CEP was stabilized with a dual feedback loop based on the f-to-2f interferometer technique[15–17], at the initial seed laser oscillator and directly after the filament compressor because the CEP is maintained during the compression stages[31]. The linearly polarized pulses before the quarter-wave plate were fully characterized with a single-shot SPIDER set-up[32]. Close to circularly polarized light was obtained with an ultrabroadband zero-order quarter-wave plate. The electric pulse field calculated from the measured SPIDER data was numerically propagated through all of the material in the beam path, yielding a period of 2.4 fs at the peak intensity and an approximate ellipticity of $E_x(t)/E_y(t) = 0.92$. This ellipticity value is only a simple estimate because for such ultrabroadband pulses the ellipticity cannot be defined with one parameter alone. The peak intensity was calibrated with the magnitude of the final momenta of the helium ions and yielded $I_p = 3.9 \times 10^{14}$ W cm^{-2} with a maximum error of 0.6×10^{14} W cm^{-2}. The laser was focused slightly behind a gas jet target to avoid an extra CEP gradient over the measurement region caused by the π Gouy phase shift over the focus.

The CEP was slowly ramped from shot to shot such that the phase was shifted by 350° over 120 min. Ramping shot by shot instead of stepping the CEP by larger values enables integration over arbitrarily long subsets of data. For the data analysis results presented here, the full ramp data was split into 36 overlapping subsets, each corresponding to a ramp over 6.6 min or 20°. This corresponds to a shift in the offset of the angular streaking of ≈130 as.

We measured the momentum distributions of the He^+ ions with a COLTRIMS set-up[21], where the laser pulse interacts with a supersonic-cooled gas jet in a reaction chamber that is kept at a background vacuum below 5×10^{-10} mbar. Both the time of flight and the position of impact of each particle are recorded[33], yielding three-dimensional momentum distributions that contain the full kinematic information about the ionization event. We recorded 10 helium ions per second against a background of ≈300 events s^{-1} from different species. We can distinguish between the different ions by their time of flight.

Different experimental parameters add to the temporal resolution. In our case, the detector resolution was about 3°, corresponding to ≈20 as. The CEP fluctuations measured by an independent f-to-2f interferometer[31] had a width of ≈40 as. The temperature of the helium target of 2.8 K caused a radial and

angular broadening of the momentum distribution as shown in Fig. 2a, adding an uncertainty of 52 as.

MOLECULAR-CLOCK TYPE OF EXPERIMENTS

Mapping through angular streaking is only unique within one optical cycle. With ultrashort pulses in the two-optical-cycle regime, it can be combined with an energy streaking by also measuring the magnitude of the streaking by the field, extending the unique mapping over more than one cycle. Attosecond angular streaking could also be combined with a pump–probe method to yield both a fast time measurement as the 'minute hand' of a clock through angular streaking and an extra coarser femtosecond time resolution from the pump–probe acting as the 'hour hand': such a scheme has been proposed for a 'molecular-clock'-type experiment where circularly polarized light induces sequential double ionization[34]. Here, we would combine attosecond angular streaking of the two photo-ionized electrons with the wave packet vibration to extend our accessible time span. The molecular clock uses the kinetic energy release of the Coulomb exploding protons as the 'hour hand' with femtosecond resolution and angular streaking determines the angle between the electron momenta as the 'minute hand' with attosecond accuracy. A first molecular-clock experiment was demonstrated in hydrogen using linearly polarized light[35]. The timing was determined by the vibrational wave-packet motion that maps time to potential energy with an oscillation period of about 16 fs. Thus, the pulse duration of the intense infrared pulse needs to be shorter than 8 fs to obtain unique results. The exact position of the vibrational wave packet when the second electron is released determines the kinetic energy release of the two protons after rapid Coulomb explosion. The time resolution of this molecular clock is however fundamentally limited to about 1.3 fs owing to the spread of the vibrational wave packet.

Received 16 January 2008; accepted 1 May 2008; published 30 May 2008.

References

1. Steinmeyer, G., Sutter, D. H., Gallmann, L., Matuschek, N. & Keller, U. Frontiers in ultrashort pulse generation: Pushing the limits in linear and nonlinear optics. *Science* **286**, 1507–1512 (1999).
2. Paul, P. M. *et al.* Observation of a train of attosecond pulses from high harmonic generation. *Science* **292**, 1689–1692 (2001).
3. Drescher, M. *et al.* Time-resolved atomic inner-shell spectroscopy. *Nature* **419**, 803–807 (2002).
4. Sansone, G. *et al.* Isolated single-cycle attosecond pulses. *Science* **314**, 443–446 (2006).
5. Kienberger, R. *et al.* Atomic transient recorder. *Nature* **427**, 817–821 (2006).
6. Dietrich, P., Krausz, F. & Corkum, P. B. Determining the absolute carrier phase of a few cycle laser pulse. *Opt. Lett.* **25**, 16–18 (2000).
7. Baker, S. *et al.* Probing proton dynamics in molecules on an attosecond time scale. *Science* **312**, 424–427 (2006).
8. Kienberger, R. *et al.* Steering attosecond electron wave packets with light. *Science* **297**, 1144–1148 (2002).
9. Goulielmakis, E. *et al.* Direct measurement of light waves. *Science* **305**, 1267–1269 (2004).
10. Itatani, J. *et al.* Attosecond streak camera. *Phys. Rev. Lett.* **88**, 173903–173906 (2002).
11. Keldysh, L. V. Ionization in the field of a strong electromagnetic wave. *Sov. Phys. JETP* **20**, 1307–1314 (1965).
12. Uiberacker, M. *et al.* Attosecond real-time observation of electron tunnelling in atoms. *Nature* **446**, 627–632 (2007).
13. Bobroff, N. Position measurement with a resolution and noise-limited instrument. *Rev. Sci. Instrum.* **57**, 1152–1157 (1986).
14. Yildiz, A. *et al.* Myosin V Walks Hand-Over-Hand: Single fluorophore imaging with 1.5-nm localization. *Science* **300**, 2061–2065 (2003).
15. Telle, H. R. *et al.* Carrier-envelope offset phase control: A novel concept for absolute optical frequency measurement and ultrashort pulse generation. *Appl. Phys. B* **69**, 327–332 (1999).
16. Jones, D. J. *et al.* Carrier-envelope phase control of femtosecond mode-locked lasers and direct optical frequency synthesis. *Science* **288**, 635–639 (2000).
17. Apolonski, A. *et al.* Controlling the phase evolution of few-cycle light pulses. *Phys. Rev. Lett.* **85**, 740–743 (2000).
18. Martiny, Ch. P. J. & Madsen, L. B. Symmetry of carrier-envelope phase difference effects in strong-field, few-cycle ionization of atoms and molecules. *Phys. Rev. Lett.* **97**, 093001 (2006).
19. Gallmann, L. *et al.* Characterization of sub-6-fs optical pulses with spectral phase interferometry for direct electric-field reconstruction. *Opt. Lett.* **24**, 1314–1316 (1999).
20. Hauri, C. P. *et al.* Generation of intense, carrier-envelope phase-locked few-cycle laser pulses through filamentation. *Appl. Phys. B* **79**, 673–677 (2004).
21. Ullrich, J. *et al.* Recoil-ion and electron momentum spectroscopy: Reaction-microscopes. *Rep. Prog. Phys.* **66**, 1463–1545 (2003).
22. Lewenstein, M., Balcou, Ph., Ivanov, M. Yu., L'Huillier, A. & Corkum, P. B. Theory of high-harmonic generation by low-frequency laser fields. *Phys. Rev. A* **49**, 2117–2132 (1994).
23. Delone, N. B. & Krainov, V. P. Energy and angular electron spectra for the tunnel ionization of atoms by strong low-frequency radiation. *J. Opt. Soc. Am. B* **8**, 1207–1211 (1991).
24. Ammosov, M. V., Delone, N. B. & Krainov, V. P. Tunnel ionization of complex atoms and of atomic ions in an alternating electromagnetic field. *Sov. Phys. JETP* **64**, 2008–2013 (1986).
25. Büttiker, M. & Landauer, R. Traversal time for tunneling. *Phys. Rev. Lett.* **49**, 1739–1742 (1982).
26. Büttiker, M. Larmor precession and the traversal time for tunneling. *Phys. Rev. B* **27**, 6178–6188 (1983).
27. Paulus, G. G. *et al.* Measurement of the phase of few-cycle laser pulses. *Phys. Rev. Lett.* **91**, 253004–253007 (2003).
28. Milošević, D., Paulus, G. G. & Becker, W. High-order above-threshold ionization with few-cycle pulse: A meter of the absolute phase. *Opt. Express* **11**, 1418–1429 (2003).
29. Constant, E., Taranukhin, V. D., Stolow, A. & Corkum, P. B. Methods for the measurement of the duration of high-harmonic pulses. *Phys. Rev. A* **56**, 3870–3878 (1997).
30. Zhao, Z. X., Chang, Z., Tong, X. M. & Lin, C. D. Circularly-polarized laser-assisted photoionization spectra of argon for attosecond pulse measurements. *Opt. Express* **13**, 1966–1977 (2005).
31. Guandalini, A. *et al.* 5.1 fs pulses generated by filamentation and carrier envelope phase stability analysis. *J. Phys. B* **39**, S257–S264 (2006).
32. Kornelis, W. *et al.* Single-shot kilohertz characterization of ultrashort pulses by spectral phase interferometry for direct electric-field reconstruction. *Opt. Lett.* **28**, 281–283 (2003).
33. Jagutzki, O. *et al.* A broad-application microchannel-plate detector system for advanced particle or photon detection tasks: Large area imaging, precise multi-hit timing information and high detection rate. *Nucl. Instrum. Methods A* **477**, 244–249 (2002).
34. Staudte, A. Thesis, Univ. Frankfurt (2005), <http://www.atom.uni-frankfurt.de/web/publications/files/AndreStaudte2005.pdf>.
35. Niikura, H. *et al.* Sub-laser-cycle electron pulses for probing molecular dynamics. *Nature* **417**, 917–922 (2002).

Supplementary Information accompanies this paper on www.nature.com/naturephysics.

Acknowledgements

This work was supported by NCCR Quantum Photonics (NCCR QP), research instruments of the Swiss National Science Foundation (SNSF), the A.-v.-H. Stiftung, the Studienstiftung des deutschen Volkes and the Deutsche Forschungsgemeinschaft. We gratefully acknowledge stimulating discussions with P. B. Corkum and M. Büttiker.

Author information

Reprints and permission information is available online at http://npg.nature.com/reprintsandpermissions. Correspondence and requests for materials should be addressed to P.E.